Measurement of Tree Height and DBH in Urban Areas Using RTK-Enabled Smartphones

Mustafa Zeybek¹

¹ Selcuk University, Güneysınır Vocational School, Güneysınır, Konya, Türkiye - (mzeybek@selcuk.edu.tr)

Keywords: Urban forestry, RTK-enabled smartphone, DBH measurement, tree height, photogrammetry, mobile mapping

Abstract

Accurate, rapid, and cost-effective measurement of biometric parameters such as diameter at breast height (DBH) and tree height is crucial for urban forestry inventories. While traditional field methods and mobile LiDAR systems offer high accuracy, their cost often limits accessibility. This study explores the applicability of real-time kinematic (RTK)-enabled smartphones as an alternative for urban tree inventory measurements. Data collected with an iPhone 14 Pro in Selçuklu, Konya, Turkey, were compared against high-accuracy reference point cloud data from a Riegl VMX mobile LiDAR system. To improve positional accuracy, an ArduSimple handheld GNSS receiver integrated with the TUSAGA-Aktif CORS-TR network was employed, and a structure-frommotion workflow was used to process smartphone imagery. The results demonstrate that RTK-enabled smartphones can achieve strong agreement with LiDAR-based measurements, supported by high correlation coefficients for both DBH and tree height. These findings suggest that smartphones, when combined with RTK corrections, provide a practical, economical, and reliable alternative for urban tree inventories, though limitations remain in small-diameter tree measurements due to error margins of approximately ± 10 cm.

1. Introduction

In recent years, specialized measurement techniques, instruments, and software have been developed to collect essential inventory data of trees. These instruments are primarily terrestrial surveying systems (Zeybek, 2025), which often provide very high accuracy and resolution but come with considerable costs. Alongside these professional systems, studies in the literature have investigated whether widely available smartphones can serve the same purpose, and promising results have been reported. Mobile applications designed for tree and forest stock inventories have also been developed, though many remain under active improvement (Schweizer et al., 2024). Furthermore, comparing the data obtained from smartphones with those acquired through conventional or advanced methods has demonstrated the stability and reliability of smartphone-based measurements. This approach enables practitioners to benefit from the accessibility of smartphones—devices available to nearly everyone worldwide—rather than relying solely on expensive equipment.

In many countries, the use of smartphones to determine tree and stock indicators and to map trees has not yet been sufficiently tested. Therefore, the aim of this study is to investigate the potential use of smartphones and to define a specific workflow for obtaining the most critical parameters in tree inventories—diameter at breast height (DBH) and tree height (Shen et al., 2023). In this way, the study seeks to reveal the inventory information of trees located in urban areas and to contribute to urban mapping practices.

Smartphone-based forest inventory methods integrate RGB cameras, LiDAR sensors, and deep learning algorithms to enable the rapid and cost-effective acquisition of individual tree biometric parameters such as diameter at breast height (DBH), height, volume, and carbon stocks (Ahamed et al., 2023, Xuan et al., 2022). For example, in the study by (Sae-ngow et al., 2025), the Arboreal Tree Height application demonstrated high correlations in both DBH and height measurements. Similarly, comparative evaluations of mobile applications such as

Arboreal, Katam, and Trestima have shown that diameter and volume measurements are largely consistent with traditional approaches, although their accuracy varies depending on terrain flatness and forest structure (Sandim et al., 2023). Another deep learning-based approach estimated DBH by segmenting tree stems from dual smartphone images, achieving an error rate below 2.5% (Khan et al., 2024). In a broader context, mobile devices equipped with RGB cameras and LiDAR are considered critical for improving measurement accuracy and accessibility; however, the lack of standardization across devices and algorithms, as well as variations in performance between devices, remains a significant challenge (Magnuson et al., 2024).

The study focuses on measuring the diameter at breast height (DBH) and height of plane trees (Platanus sp.) located in the central median of Yeni İstanbul Avenue in the Selçuklu District of Konya. Plane trees, one of the most commonly used species in urban landscaping projects across Turkey, are particularly preferred along roadsides, parks, and medians due to their rapid growth and broad canopy. In urban ecological balance, plane trees play vital roles: their large leaf surfaces capture dust and harmful particulates, thereby improving air quality, while sequestering carbon and increasing oxygen production. By providing broad shade and facilitating evapotranspiration, they help create cooling microclimates, mitigate the urban heat island effect, and contribute to energy savings. Additionally, they absorb noise, enhance aesthetic appeal, and provide habitats for birds and insects, thereby supporting biodiversity. Their root systems prevent erosion and improve stormwater infiltration, strengthening urban water management. In median strips and along roadsides, plane trees filter pollution generated by traffic and provide shade and comfort for pedestrians, ultimately making city life healthier and more sustainable (Güneş et al., 2022).

Data collection was carried out in August 2025 using two different methods: (1) a mobile LiDAR system and (2) an iPhone 14 Pro smartphone. To evaluate the accuracy of the smartphone-

derived results, the mobile LiDAR system, which provides high-precision reference data, was used as the benchmark. In the study, the DBH values measured at $1.3\,\mathrm{m}$ height and the maximum Z (AGL) values obtained from the smartphone data were taken as the primary parameters. The distribution of tree diameters derived from the smartphone was found to be largely consistent with the distribution obtained from the MLS method. These findings indicate that smartphone-based applications hold strong potential to serve as an effective alternative to traditional methods in the future.

1.1 Motivation and Contribution

In this context, the integration of GNSS RTK with smartphones emerges as a critical contribution of this study. One of the major limitations of smartphone-based measurements is the lack of positional accuracy. While conventional smartphone measurements using camera- and sensor-based methods can estimate DBH and tree height, geodetic-level positioning of the derived data is often not achievable. This shortcoming particularly hinders the accurate mapping of tree spatial distributions in urban areas and their reliable integration into GIS-based analyses. The integration of an RTK-enabled GNSS device bridges this gap by linking smartphone-acquired imagery with centimeter-level precise coordinates. In this way, the accessibility and cost-effectiveness of smartphones are preserved, while providing positional accuracy comparable to high-cost systems such as LiDAR, thereby making the approach applicable to both academic research and practical applications.

2. Methodology

2.1 ArduSimple RTK Handheld Surveyor Kiti ile GNSS Destekli Ölçümler

In the photogrammetric workflow, the accuracy of camera positions was enhanced using the ArduSimple RTK Handheld Surveyor Kit (ArduSimple, 2025) (Figure 1). This device, equipped with an RTK-based GNSS receiver, provides centimeter-level positioning accuracy (İbrahim Murat Ozulu et al., 2024). Systems designed for geodetic purposes are also capable of producing centimeter-level precision when employed for RTK applications (Konakoğlu and Şenses, 2023). During fieldwork, GNSS measurements obtained from the device were integrated into the image position data used in Agisoft Metashape, thereby improving the overall model accuracy.

Considering that camera position errors were calculated as 2.46 cm, 4.07 cm, and 3.46 cm along the X, Y, and Z axes, respectively, the RTK-supported GNSS measurements made a significant contribution to reducing these errors. In addition, the ArduSimple device facilitated the transformation of positional data into the TUREF / TM33 (EPSG:5255) coordinate system for use in GIS-based analyses.

The integration of the ArduSimple RTK Handheld Surveyor Kit not only increased the accuracy of camera position information but also strengthened the geodetic reliability of the derived point cloud and digital elevation model.

The ArduSimple RTK Handheld Surveyor Kit provides GNSS data in compliance with the NMEA0183 standard (NMEA, 2018). These messages include information on position, time, velocity, and accuracy indicators. The main NMEA sentences and their mathematical formulations, as also described in (Misra and Enge, 2011), are summarized below.



Figure 1. System configuration used in the study.

GGA – Global Positioning System Fix Data Provides latitude, longitude, and ellipsoidal height information:

$$P = (\phi, \lambda, h), \qquad h = h_{\text{ellipsoid}} + N$$
 (1)

where ϕ is latitude, λ is longitude, h represents ellipsoidal height, and N denotes the geoid undulation.

RMC – Recommended Minimum Specific GNSS Information Contains ground speed and heading information:

$$v_N = v \cdot \cos(\theta), \qquad v_E = v \cdot \sin(\theta)$$
 (2)

where v is ground speed and θ is the course angle.

GSA – GNSS DOP and Active Satellites Provides DOP (Dilution of Precision) values based on satellite geometry:

$$\sigma_{\text{position}}^2 = DOP^2 \cdot \sigma_{UERE}^2 \tag{3}$$

where σ_{UERE} represents the User Equivalent Range Error.

VTG – Course and Ground Speed Expresses the velocity vector with North and East components:

$$\vec{v} = (v_N, v_E), \qquad |\vec{v}| = \sqrt{v_N^2 + v_E^2}$$
 (4)

ZDA – Time and Date GPS time is converted to UTC:

$$t_{UTC} = t_{GPS} - \Delta t_{\text{leap}} \tag{5}$$

In summary, the NMEA messages provided by the ArduSimple RTK Handheld Surveyor Kit deliver geographic coordinates (ϕ, λ, h) , velocity vectors (v_N, v_E) , DOP-based accuracy measures, and precise time information, thereby supplying the essential input required for real-time positioning techniques such as PPP-RTK and CORS-based RTK.

Network RTK (NRTK) represents an enhanced version of the classical RTK approach (Hofmann-Wellenhof et al., 2008). In-

stead of relying on a single reference station, multiple permanent GNSS reference stations distributed across a region are employed. These stations transmit real-time GNSS observations to a central server, where ionospheric, tropospheric, and satellite clock/orbit errors are modeled at the network level. The resulting corrections are then disseminated to users, typically via the NTRIP protocol (Networked Transport of RTCM via Internet Protocol). The principal advantage of Network RTK lies in its ability to mitigate distance-dependent errors, which increase with baseline length in single-station RTK, by using regional error modeling.

Continuously Operating Reference Stations (CORS) are networks of permanent GNSS reference stations integrated into national geodetic frameworks, providing 24/7 GNSS data streams. These data are made available to users in real time (RTCM format) or for post-processing (RINEX format), enabling centimeter-level positioning accuracy through DGNSS, RTK, and Network RTK solutions (Bakıcı and Mekik, 2014). In Türkiye and the Turkish Republic of Northern Cyprus, the national system TUSAGA-Aktif (CORS-TR) has been operational since 2008 as a TÜBİTAK-supported public project, operated by the General Directorate of Land Registry and Cadastre (TKGM). GNSS data collected by the reference stations are processed at the control center and distributed to users as RTCM/NTRIP corrections, thereby facilitating cadastral and geodetic tasks in a faster, more economical, and more reliable manner. By 2013, the performance of approximately 4,610 GNSS receivers had improved by 50%, contributing to cadastral renewal projects valued at 220 million USD and generating savings of around 35 million USD, which enabled the system to amortize its investment cost within the first year (Bakıcı and Mekik, 2014). More recently, the modernization of software and hardware infrastructure has aimed to establish a brand-independent, flexible, and sustainable architecture for TUSAGA-Aktif (Aydın et al., 2025).

2.2 SWMAPS

In this study, GNSS track point data collected using the SW Maps software (Softwel, 2025) were processed to enable both visualization and conversion into an analysis-ready format. First, the data obtained in Excel format were imported into the R environment, and the Latitude, Longitude, and Elevation values were converted into numeric form. These coordinates were then transformed into a GIS-compatible sf object and reprojected from the WGS84 coordinate system (EPSG:4326) to the Turkish National Reference System, EPSG:5255. The transformed coordinates were appended to the dataset, and the resulting points were visualized on an interactive map using the Leaflet library. Finally, GNSS points along with their timestamps, elevation, and horizontal/vertical accuracy values were exported in XLSX/CSV format (Algorithm 1). This workflow preserved the temporal dimension while producing a spatially accurate dataset ready for further analysis.

In the measurements conducted through the SW Maps application, the TUSAGA-Aktif CORS system was employed. Within the application, the NTRIP (Networked Transport of RTCM via Internet Protocol) (Hofmann-Wellenhof et al., 2008) client was activated, and the relevant user credentials and mountpoint settings were entered to receive real-time correction data from the GNSS receiver via the internet. Thanks to the continuously operating reference stations provided by TUSAGA-Aktif, positional accuracy was reduced to the centimeter level, enabling

Algorithm 1 Processing workflow for converting SW Maps track points into EPSG:5255 with timestamp preservation

- Input: GNSS track point data exported from SW Maps in Excel format (TRACK_POINTS sheet)
- 2: **Output:** Time-stamped GNSS dataset in EPSG:5255 and exported CSV/XLSX file
- 3: Import the Excel sheet into a dataframe → gnss_df
- 4: Convert Latitude, Longitude, and Elevation values to numeric format
- 5: Generate an sf object using (Lon, Lat) coordinates in WGS84 (EPSG:4326)
- Reproject the coordinates into the Turkish National Reference System (EPSG:5255)
- 7: Append the transformed X_{5255}, Y_{5255} values to the data-frame
- 8: Visualize the points interactively using the Leaflet library
- 9: Export the enhanced dataset (Time, Lat, Lon, Elevation, Horizontal/Vertical Accuracy, X_{5255}, Y_{5255}) as CSV/XLSX

the acquisition of reliable and precise coordinates, particularly for urban inventory studies (Öcalan and Soycan, 2012). Consequently, the data recorded through SW Maps were supported by both differential GNSS and RTK corrections, thereby enhancing the accuracy and reliability of the inventory measurements.

2.3 HEIC to JPG

This study addresses the conversion of images captured in the HEIC format by iPhone devices—unsupported by Agisoft software—into the JPEG format, while simultaneously enriching them with high-precision GNSS data. In the first step, GNSS records containing latitude, longitude, elevation, and timestamps were read, cleaned, and converted into POSIX format within the local time zone. Subsequently, the EXIF creation time of each HEIC file was extracted, and the image was matched with the nearest GNSS record within a predefined threshold (e.g., 3 seconds). When a match was found, the HEIC file was converted into JPEG format, with the original EXIF information (e.g., camera parameters, image resolution) preserved. The updated GNSS coordinates and corrected timestamp were then embedded into the metadata of the resulting JPEG image (Algorithm 2).

2.4 Agisoft Metashape Processing and Data Handling

Following the field survey, the acquired images (Figure 2) were processed using *Agisoft Metashape Professional* software (version 2). In total, 272 images captured with the iPhone 14 Pro camera at an average acquisition distance of 19.3 m were processed, resulting in a ground sampling distance (GSD) of 6.93 mm/pixel. All images were successfully aligned, producing 144,143 tie points and 367,552 projections. The mean reprojection error was calculated as 0.928 pixels.

During camera calibration, the iPhone 14 Pro rear camera system was modeled with a focal length of 6.9 mm and a pixel size of 2.47 μ m. Additionally, distortion parameters (k_1 , k_2 , k_3 , k_4 , p_1 , p_2) were optimized. The positioning accuracy of the reconstructed camera poses was estimated as 2.46 cm, 4.07 cm, and 3.46 cm along the X, Y, and Z axes, respectively, yielding an overall mean error of 5.88 cm.

Dense point cloud generation was performed using depth maps, producing a total of 26,344,790 points (Figure 2). The reported coordinate precision of the point cloud was 3.46 mm. A

Algorithm 2 HEIC to JPEG Conversion with GNSS EXIF Matching

```
1: Input: GNSS CSV file (time-stamped), HEIC image folder
   Output: JPEG images with copied EXIF and updated
   GNSS metadata
   Read GNSS CSV file and clean timestamps
   Convert GNSS timestamps to POSIX format in local
   List all HEIC files in input directory
6: if no HEIC files found then
       Stop execution with error
8:
   end if
9.
   Initialize progress
10: for each HEIC file do
       Extract base name and prepare JPEG output path
11:
12:
       if JPEG already exists with EXIF metadata then
13:
           Stop processing for safety
14:
       Read EXIF metadata from HEIC file
15:
       if no valid timestamp found in EXIF then
16:
           Skip file
17:
18:
       end if
       Convert EXIF timestamp to POSIX
19:
       Find closest GNSS record based on timestamp differ-
20:
21:
       if no GNSS match within max difference threshold
   then
22:
           Skip file
23:
       end if
24:
       Convert HEIC file to JPEG
       Copy all EXIF data from HEIC to JPEG
25:
                                                     GNSS
26:
       Overwrite DateTimeOriginal and insert
   metadata (lat, lon, alt, refs)
       Update progress
28:
   end for
   Stop and report number of processed files and total duration
```

Digital Elevation Model (DEM) was generated, and the dataset was transformed into the Turkish National Reference Frame, TUREF / TM33 (EPSG:5255) coordinate system.

The total data processing time was recorded as 13 minutes and 7 seconds, while dense point cloud generation required 6 minutes and 55 seconds. All processing was performed on a system equipped with a 12th Generation Intel(R) Core(TM) i7-12700H processor, 15.73 GB RAM, and an Intel(R) Iris(R) Xe Graphics GPU.

Algorithm 3 DBH and Height Extraction from Point Cloud

```
1: Input: Raw point cloud LAS_{raw}
    Output: Tree table \{X, Y, DBH, Height, RMSE\}
    Classify noise \rightarrow remove
   Classify ground with CSF \rightarrow DTM
   Normalize heights: LAS_{norm} = LAS_{raw} - DTM
Extract slice at 1.25 < Z < 1.35 m
6.
    Cluster slice with DBSCAN
7:
8:
   for each cluster C_i do
        Fit circle \rightarrow (cx, cy, r)
9:
        Compute RMSE
10:
11:
        if RMSE > 0.07 m or r > 0.5 m then skip
12:
        else
            DBH = 2r \times 100 \text{ cm}
13:
            Height = max(Z) inside buffer
14:
15:
            Save (cx, cy, DBH, Height, RMSE)
        end if
16:
17:
   end for
18: Export results to CSV
```

The proposed approach (Algorithm 3) is a scientific method designed to extract fundamental dendrometric parameters, such

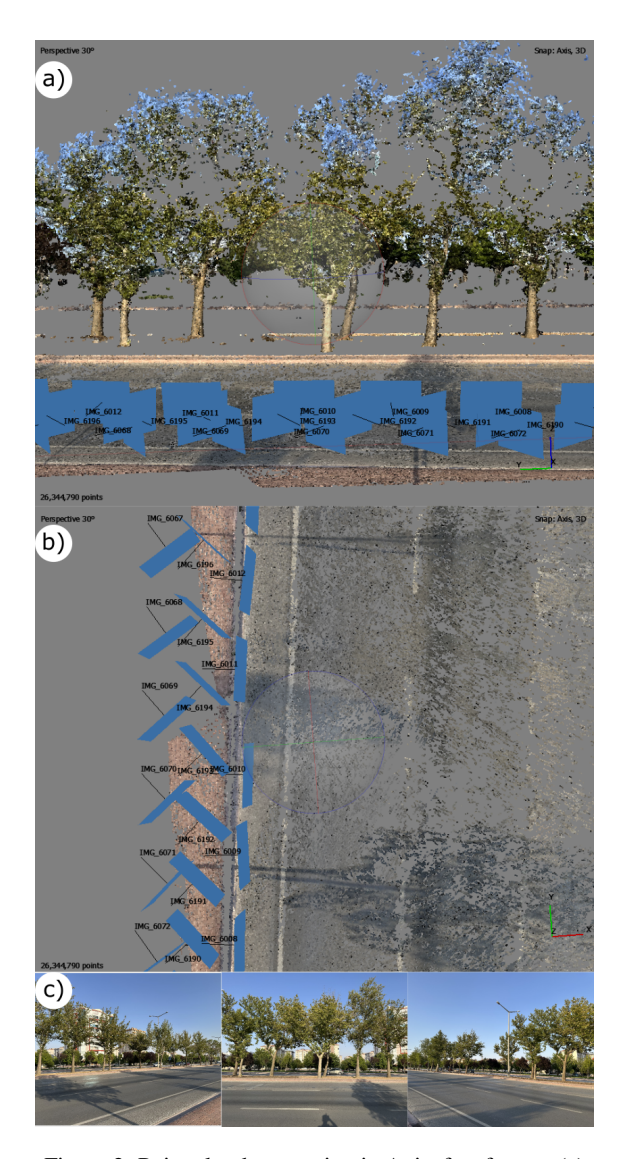


Figure 2. Point cloud generation in Agisoft software. (a) Perspective view of the tree point cloud representation, (b) side view illustrating camera positions and the generated dense point cloud, (c) original field photographs. The blue rectangles represent camera locations, while the three-dimensional point cloud clearly depicts the trunk and crown structures of the trees in detail.

as diameter at breast height (DBH) and tree height, from point clouds. The process begins with the removal of noise points from the raw point cloud, followed by ground classification, during which a Digital Terrain Model (DTM) is generated and subsequently used for height normalization. After normalization, a horizontal slice is extracted at the range 1.25 < Z < 1.35 m, which corresponds to the DBH measurement height.

In the next step, the points within the slice are clustered using the density-based clustering algorithm DBSCAN, where each cluster corresponds to an individual tree stem. A circle is then fitted to each cluster to estimate the stem center (c_x,c_y) and radius r. The quality of the fitted circle is evaluated using the root mean square error (RMSE); clusters exceeding the defined thresholds $(RMSE>0.07~{\rm m~or}~r>0.5~{\rm m})$ are discarded. For the accepted clusters, DBH is calculated using the formula $DBH=2r\times100~{\rm cm}$, while tree height is determined as the maximum Z value within a buffer defined around the stem

center. The results, including stem center coordinates, DBH, height, and error metrics, are recorded in a table.

This methodology enables reliable and repeatable extraction of individual tree parameters from point cloud data, providing an effective measurement tool for forestry and ecological research (Vatandaslar and Zeybek, 2020, Vatandaslar and Zeybek, 2021, Zeybek and Vatandaslar, 2021, Zeybek, 2025).

2.5 Ground truth Dataset

In this study, the accuracy of the proposed methods was evaluated using ground truth data obtained from the Riegl VMX mobile LiDAR system. The Riegl VMX is a mobile mapping solution renowned for its capability to produce high-density and highly accurate three-dimensional point clouds. The data acquired from this system were comparatively assessed against the point clouds processed in the study, enabling a quantitative validation of the model's performance. Consequently, the reliability of the proposed approach was tested using an independent, high-precision LiDAR source, thereby supporting the validity and robustness of the results.

3. Comparison of LiDAR and Agisoft Point Cloud Data

In this study, mobile LiDAR system measurements of stem center coordinates (c_x, c_y) , diameter at breast height (DBH), and tree height were compared against values derived from point clouds generated using Agisoft Metashape software. The comparison procedure is summarized below.

3.1 Data Matching

For each tree, the center coordinates (c_x, c_y) obtained from LiDAR data were matched with the nearest stem center detected in the Agisoft point cloud. The Euclidean distance approach was applied:

$$d = \sqrt{(c_{x,L} - c_{x,A})^2 + (c_{y,L} - c_{y,A})^2}$$
 (6)

where $c_{x,L},c_{y,L}$ represent the LiDAR-derived coordinates, and $c_{x,A},c_{y,A}$ denote the coordinates calculated from the Agisoft point cloud.

3.2 DBH Comparison

For each tree, DBH values obtained from both methods were compared. The error term was calculated as:

$$\Delta DBH = DBH_{LiDAR} - DBH_{Agisoft} \tag{7}$$

3.3 Height Comparison

Tree height was determined using the maximum Z value extracted from both the LiDAR and Agisoft point clouds. The difference was expressed as:

$$\Delta H = H_{LiDAR} - H_{Agisoft} \tag{8}$$

3.4 Statistical Analysis

To evaluate the agreement between LiDAR measurements and the smartphone-based photogrammetric method, several error metrics were calculated. These included bias (mean error), root mean square error (RMSE), standard deviation (SD), mean absolute error (MAE), and Bland–Altman limits of agreement (LoA). Additionally, the strength of the relationship between methods was quantified using the Pearson correlation coefficient (r) and the coefficient of determination (R^2) . The relevant statistical measures are defined as follows:

$$Bias = \frac{1}{n} \sum_{i=1}^{n} (X_{LiDAR,i} - X_{SmartPhone,i})$$
 (9)

$$RMSE = \sqrt{\frac{1}{n} \sum_{i=1}^{n} (X_{LiDAR,i} - X_{SmartPhone,i})^2} \quad (10)$$

$$MAE = \frac{1}{n} \sum_{i=1}^{n} |X_{LiDAR,i} - X_{SmartPhone,i}|$$
 (11)

4. Results

In this study, the diameter at breast height (DBH) and tree height values obtained from LiDAR data were compared with those derived from the smartphone-based photogrammetric method. For the comparison, tree center coordinates were used as the basis, and a nearest-neighbor algorithm was applied. Matches were considered valid only when the distance between centers was less than 0.5 m and the mutual nearest-neighbor condition was satisfied. To minimize the influence of outliers, pairs with DBH differences exceeding $|\Delta {\rm DBH}| > 10$, cm were excluded from the analysis.

After this filtering, a total of 27 tree matches were evaluated. As summarized in Table 1 and Table 2, the statistical results indicated a strong level of agreement between LiDAR and smartphone-based measurements.

Table 1. Error metrics of LiDAR and smartphone measurements ($|\Delta DBH| \le 10$ cm).

Metric	n	Bias	SD	MAE	RMSE
DBH (cm)	27	0.580	5.03	4.48	4.97
Height (m)	27	0.230	1.62	1.17	1.61

Table 2. Correlation coefficients and limits of agreement (LoA) between LiDAR and smartphone measurements ($|\Delta DBH| \leq 10$ cm).

Metric	LoA (Lower–Upper)	r	R^2	p
DBH (cm)	-9.27 – 10.40	0.836	0.698	0.555
Height (m)	-2.95 - 3.41	0.888	0.788	0.466

When examining Table 1 and Table 2, it is evident that the measurements obtained from LiDAR and the smartphone-based photogrammetric approach exhibit a generally high level of agreement.

For DBH results, the mean difference (Bias) was found to be $0.58, \mathrm{cm}$, indicating that the systematic deviation between the two methods was very small. The standard deviation (SD) was

5.03, cm and the RMSE was 4.97, cm, suggesting that the error distribution was confined within a relatively narrow range. The mean absolute error (MAE) was similarly low at 4.48, cm. According to the Bland–Altman analysis (Bland and Altman, 1986), the limits of agreement (LoA) ranged from -9.27 to +10.40, cm, demonstrating that most measurement differences remained within a ± 10 , cm interval. Furthermore, the correlation coefficient (r=0.836) and the coefficient of determination ($R^2=0.698$) indicated a strong relationship between the two methods. The p-value (p=0.555) confirmed that the observed differences were not statistically significant, implying that the discrepancies were within a random error level.

Regarding tree height results, the mean difference was $0.23,\,\mathrm{m}$, suggesting almost no systematic bias between the LiDAR and smartphone-based measurements. The SD $(1.62,\mathrm{m}),\,\mathrm{RMSE}$ $(1.61,\mathrm{m}),\,\mathrm{and}\,\mathrm{MAE}\,(1.17,\mathrm{m})$ further indicated that the discrepancies between the two methods were relatively small. The Bland–Altman limits of agreement, ranging from -2.95 to $+3.41,\,\mathrm{m},\,\mathrm{showed}$ that the majority of measurements fell within a $\pm 3,\,\mathrm{m}$ interval. The correlation coefficient (r=0.888) and $R^2=0.788$ confirmed a very strong relationship, while the non-significant $p\text{-value}\,(p=0.466)$ demonstrated that the differences between the two measurement approaches were not statistically meaningful, thus supporting the consistency and reliability of the smartphone-based measurements.

Overall, the low bias, low RMSE, and high correlation coefficients for both DBH and tree height demonstrate that the smartphone-based photogrammetric method produces results that are highly consistent with LiDAR measurements. In particular, the lower error values and higher correlation observed for tree height measurements indicate that this approach can be confidently applied in field studies. Nevertheless, the observed error margin of $\pm 10~\rm cm$ for DBH measurements should be carefully considered, especially in studies involving small-diameter trees where higher sensitivity is required.

When examining Figures 3 and 4, it becomes evident that both DBH and tree height measurements obtained from LiDAR and smartphone-based methods exhibit strong correlations. The 1:1 reference lines confirm that the two approaches are generally consistent in their overall trends, while the Bland–Altman analyses reveal individual measurement differences of up to $\pm 10~\rm cm$. The error histograms show that the residuals are largely concentrated around zero, indicating no systematic bias between the methods. Furthermore, the comparison of tree center coordinates demonstrates strong spatial agreement between the two datasets, although minor positional shifts are present. Collectively, these findings support the conclusion that low-cost smartphone-based measurements can provide a practical and reliable alternative to LiDAR data in field applications.

Table 3. Distance statistics (m) of tree center positions derived from LiDAR and smartphone (Agisoft) point clouds.

\overline{n}	Mean	Std. Dev.	Min.	Q1	Media	n Q3	Max.
27	0.126	0.043	0.069	0.097	0.116	0.156	0.238

According to the results summarized in Table 3, the mean positional difference between tree centers derived from LiDAR and smartphone-based point clouds was approximately 0.126, m. The standard deviation of 0.043, m indicates that the discrepancies were concentrated within a relatively narrow range. The minimum difference was 0.069, m, while the maximum reached

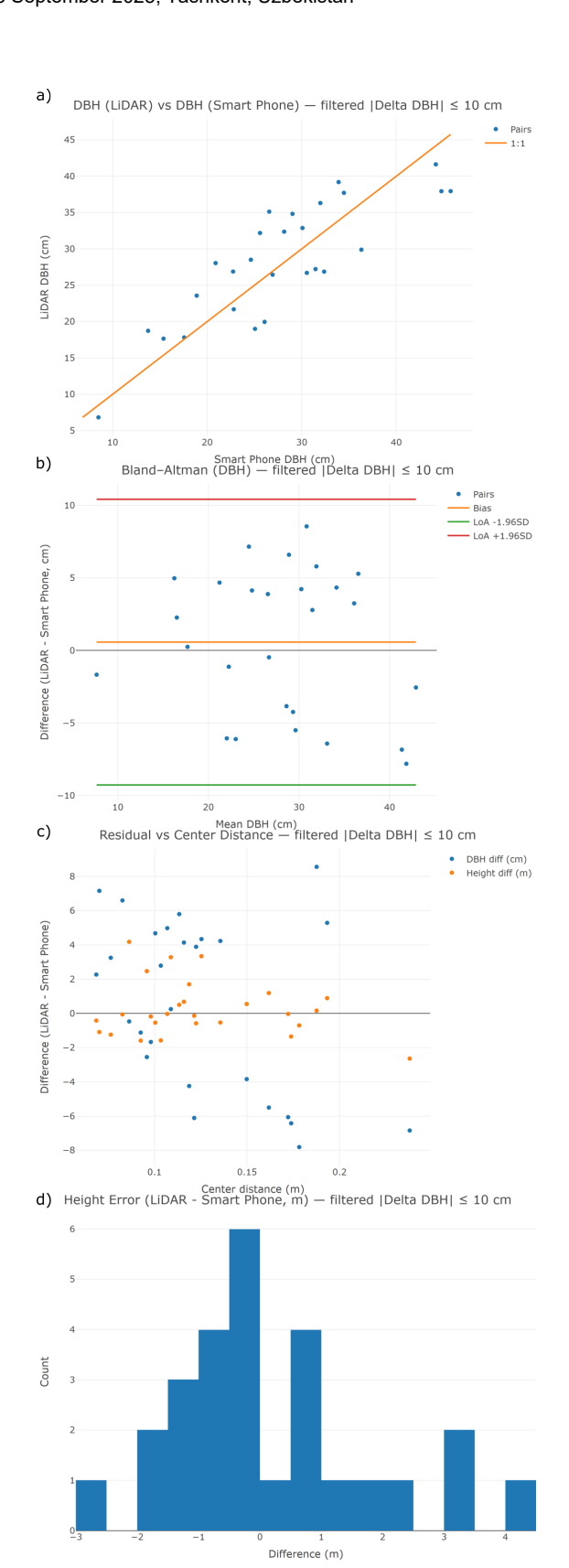


Figure 3. Comparison of DBH and tree height measurements obtained from LiDAR and smartphone (Agisoft) point clouds:

(a) scatter plot with 1:1 reference line for DBH, (b)

Bland–Altman difference analysis for DBH, (c) residual distribution as a function of center distance, (d) histogram of tree height errors.

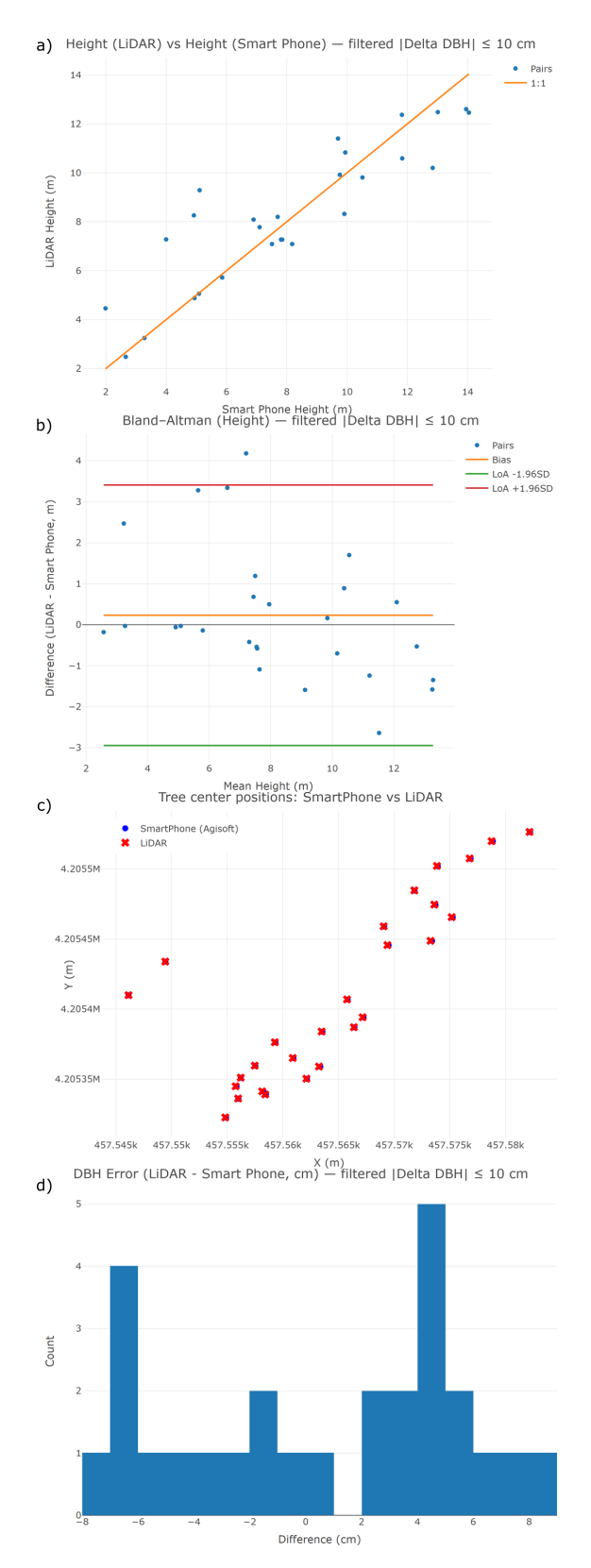


Figure 4. Additional results from LiDAR and smartphone (Agisoft) point cloud comparisons: (a) scatter plot with 1:1 reference line for tree height, (b) Bland–Altman difference analysis for tree height, (c) spatial comparison of tree center coordinates (LiDAR in red crosses, smartphone in blue dots), (d) histogram of DBH errors.

0.238, m. The median value of 0.116, m suggests that the distribution of differences was close to symmetric. These results demonstrate that low-cost smartphone-based methods can provide acceptable accuracy for determining tree center positions when compared to LiDAR.

Overall, the findings of this study indicate that RTK-enabled smartphones offer a viable and cost-effective alternative for conducting urban tree inventory studies. Nevertheless, certain limitations of the method must be acknowledged. In particular, the observed ± 10 cm error range in DBH measurements can negatively affect precision in the case of small-diameter trees. These deviations are mainly attributable to dense branches and foliage surrounding the trunk, as well as shading conditions that complicate circle fitting during photogrammetric processing. Furthermore, the limited field of view of smartphone cameras, the inability to capture images from desired positions in constrained urban environments, and variable lighting conditions may introduce photogrammetric distortions, thereby reducing measurement accuracy. From a positional perspective, although RTK corrections were applied, multipath effects caused by signal reflections in urban areas occasionally resulted in centimeter-level deviations. From a statistical standpoint, the relatively small sample size restricts the generalizability of the results to diverse tree species and structural forms. Consequently, to strengthen the reliability and validity of this approach, additional studies should be conducted across different tree types, under varying environmental conditions, and with larger datasets.

5. Conclusion

In this study, the applicability of RTK-enabled smartphones for urban tree inventory assessments was investigated. The results demonstrate that data collected with smartphones can achieve accuracy levels comparable to those obtained with high-precision mobile LiDAR systems. Considering their accessibility and low cost, smartphone-based photogrammetric approaches represent a valuable alternative for rapid and practical data acquisition in urban environments. Nevertheless, several limitations remain, including error margins that affect the precision of measurements for small-diameter trees, photogrammetric uncertainties arising from imaging conditions, and GNSS signal multipath effects in urban settings. To enhance the reliability of the method, further studies should be conducted on a wider range of tree species and sizes, under diverse environmental conditions, and with larger sample datasets. Overall, RTK-corrected smartphone measurements provide a fast, economical, and sustainable solution for urban forestry inventories and, when supported by appropriate workflows, hold strong potential for both academic research and practical applications.

Acknowledgement

This research was supported by Selçuk University Scientific Research Projects (BAP) under reference number 23401134. The author also gratefully acknowledges Koyuncu LiDAR Company for providing Mobile LiDAR mapping system VMX-450 data, which was utilized to validate and assess the quality of the proposed study results.

References

Ahamed, A., Foye, J., Poudel, S., Trieschman, E., Fike, J., 2023. Measuring Tree Diameter with Photogram-

- metry Using Mobile Phone Cameras. *Forests*, 14, 2027. https://www.mdpi.com/1999-4907/14/10/2027.
- ArduSimple, 2025. Rtk handheld surveyor kit. https://www.ardusimple.com/product/rtk-handheld-surveyor-kit/. Accessed: 2025-08-23.
- Aydın, M., Soylu, M., Ayyıldız, E., 2025. Performance evaluation of the new control center and receiver hardware for the cors-tr system. *International Archives of the Photogrammetry, Remote Sensing and Spatial Information Sciences*, XLVIII-M-6, 331–335.
- Bakıcı, S., Mekik, C., 2014. TUSAGA-Aktif: Delivering Benefits to Turkey. *Coordinates*, 10(2), 19–26.
- Bland, J. M., Altman, D. G., 1986. Statistical methods for assessing agreement between two methods of clinical measurement. *Lancet*, 1(8476), 307–310.
- Güneş, C., Önder, S., Mimarlığı, P., Ve, M., Fakültesi, T., Üniversitesi, S., Konya, T., 2022. Konya İli Meram İlçesinde Bulunan Anıt Ağaçların İncelenmesi ve Koruma Statülerinin Belirlenmesine Yönelik Bir Araştırma. *Ulusal Çevre Bilimleri Araştırma Dergisi*, 5, 100-111. https://dergipark.org.tr/tr/pub/ucbad/issue/71154/1099574.
- Hofmann-Wellenhof, B., Lichtenegger, H., Wasle, E., 2008. GNSS – Global Navigation Satellite Systems: GPS, GLONASS, Galileo, and more. 1st edn, Springer, Vienna.
- Khan, A., Nawaz, U., Ulhaq, A., Gondal, I., Javed, S., 2024. Accurate and Efficient Urban Street Tree Inventory with Deep Learning on Mobile Phone Imagery. 2023 International Conference on Digital Image Computing: Techniques and Applications, DICTA 2023, 486-493. https://arxiv.org/pdf/2401.01180.
- Konakoğlu, B., Şenses, S., 2023. Hassas Nokta Konumlama (PPP) Tekniğinin Ağaçlık Alanlardaki Konum Belirleme Performansının CSRS-PPP Yazılımı Kullanılarak İncelenmesi. *Afyon Kocatepe Üniversitesi Fen ve Mühendislik Bilimleri Dergisi*, 23(3), 730–739. https://doi.org/10.35414/akufemubid.1254856. Cited By: 1.
- Magnuson, R., Erfanifard, Y., Kulicki, M., Gasica, T. A., Tangwa, E., Mielcarek, M., Stereńczak, K., 2024. Mobile Devices in Forest Mensuration: A Review of Technologies and Methods in Single Tree Measurements. *Remote Sensing 2024, Vol. 16, Page 3570*, 16, 3570. https://www.mdpi.com/2072-4292/16/19/3570/htm https://www.mdpi.com/2072-4292/16/19/3570.
- Misra, P., Enge, P., 2011. *Global Positioning System: Signals, Measurements, and Performance*. 2nd edn, Ganga-Jamuna Press, Lincoln, MA, USA.
- NMEA, 2018. NMEA 0183 Standard for Interfacing Marine Electronic Devices. Version 4.11 edn, National Marine Electronics Association.
- Öcalan, T., Soycan, M., 2012. RTCM/SSR Mesajları İle Gerçek Zamanlı Hassas Nokta Konumlama (PPP-RTK) Tekniği. *Harita Teknolojileri Elektronik Dergisi*, 4(2), 30–41. http://www.teknolojikarastirmalar.com.
- Sae-ngow, P., Worachairungreung, M., Hemwan, P., Toathuean, N., Chimpalee, N., Kulpanich, N., 2025. Smartphone LiDAR for urban forest carbon assessment: A comparative study with traditional methods. *MethodsX*, 15, 103473. https://doi.org/10.1016/J.MEX.2025.103473.

- Sandim, A., Amaro, M., Silva, M. E., Cunha, J., Morais, S., Marques, A., Ferreira, A., Lousada, J. L., Fonseca, T., 2023. New Technologies for Expedited Forest Inventory Using Smartphone Applications. *Forests*, 14.
- Schweizer, D., Cole, R. J., Werden, L. K., Cedeño, G. Q., Rodriguez, D., Navarro, K., Esquivel, J. M., Max, S., Chiriboga, F. E., Zahawi, R. A., Holl, K. D., Crowther, T. W., 2024. Review and assessment of smartphone apps for forest restoration monitoring. *Restoration Ecology*, 32(4), e14136. https://onlinelibrary.wiley.com/doi/10.1111/rec.14136.
- Shen, Y., Huang, R., Hua, B., Pan, Y., Mei, Y., Dong, M., 2023. Automatic Tree Height Measurement Based on Three-Dimensional Reconstruction Using Smartphone. *Sensors*, 23(16), 7248. https://doi.org/10.3390/s23167248.
- Softwel, 2025. Sw maps gis & data collection application. https://play.google.com/store/apps/details?id=np.com.softwel.swmaps. Accessed: 2025-08-26.
- Vatandaslar, C., Zeybek, M., 2020. Application of handheld laser scanning technology for forest inventory purposes in the NE Turkey. *Turkish Journal of Agriculture and Forestry*, 44(3), 229–242. https://doi.org/10.3906/tar-1903-40.
- Vatandaslar, C., Zeybek, M., 2021. Extraction of forest inventory parameters using handheld mobile laser scanning: A case study from Trabzon, Turkey. *Measurement*, 177, 109328. https://doi.org/10.1016/j.measurement.2021.109328.
- Xuan, J., Li, X., Du, H., Zhou, G., Mao, F., Wang, J., Zhang, B., Gong, Y., Zhu, D., Zhou, L., Huang, Z., Xu, C., Chen, J., Zhou, Y., Chen, C., Tan, C., Sun, J., 2022. Intelligent Estimating the Tree Height in Urban Forests Based on Deep Learning Combined with a Smartphone and a Comparison with UAV-LiDAR. *Remote Sensing*, 15, 97. https://www.mdpi.com/2072-4292/15/1/97.
- Zeybek, M., 2025. Semiautomatic Diameter-at-Breast-Height Extraction from Structure-from-Motion-Based Point Clouds Using a Low-Cost Fisheye Lens. *Forests*, 16(3), 439. https://doi.org/10.3390/f16030439.
- Zeybek, M., Vatandaslar, C., 2021. An Automated Approach for Extracting Forest Inventory Data from Individual Trees Using a Handheld Mobile Laser Scanner. *Croatian Journal of Forest Engineering*, 42(3), 515–528. https://doi.org/10.5552/crojfe.2021.1096.
- İbrahim Murat Ozulu, Dilmaç, H., İlçi, V., 2024. The Accuracy Analysis and Usability of Low Cost RTK Portable Kit on Surveying Aims. 906 LNNS, Springer, 270–276.